Hindawi
Advances in Mathematical Physics
Volume 2022, Article ID 7753879, 13 pages
https://doi.org/10.1155/2022/7753879

Research Article

New Results of Some of the Conformable Models Arising in Dynamical Systems

Md Nur Alam[1], **Onur Alp Ilhan**[2], **Jalil Manafian**[3,4], **Muhammad Imran Asjad**[5], **Hadi Rezazadeh**[6] and **Haci Mehmet Baskonus**[7]

[1]*Department of Mathematics, Pabna University of Science and Technology, Pabna, 6600, Bangladesh*
[2]*Department of Mathematics and Science Education, Faculty of Education, Erciyes University, Kayseri 38039, Turkey*
[3]*Department of Applied Mathematics, Faculty of Mathematical Sciences, University of Tabriz, Tabriz, Iran*
[4]*Natural Sciences Faculty, Lankaran State University, 50, H. Aslanov str., Lankaran, Azerbaijan*
[5]*Department of Mathematics, University of Management and Technology, Lahore 54700, Pakistan*
[6]*Faculty of Engineering Technology, Amol University of Special Modern Technologies, Amol, Iran*
[7]*Department of Mathematics and Science Education, Faculty of Education, Harran University, Sanliurfa, Turkey*

Correspondence should be addressed to Md Nur Alam; nuralam.pstu23@gmail.com

Received 5 April 2022; Accepted 5 September 2022; Published 20 September 2022

Academic Editor: Jorge E. Macias-Diaz

This article investigates the new results of three nonlinear conformable models (NLCMs). To study such varieties of new soliton structures, we perform the generalized Kudryashov (GK) method. The obtained new results are defined in the styles of the exponential and rational functions. The derived new soliton structures are stable, serviceable, and fitting to embrace the conformable dynamics, chaotic vibrations, global bifurcations, optimal control problems, fluid mechanics, plasma physics, system identification, local bifurcations, control theory and resonances, and so many. The outcomes declare that the process is hugely valuable and accessible for investigating nonlinear conformable order models treated in theoretical physics.

1. Introduction

Conformable calculus is a part of an analytical investigation that scrutinizes the actual or complicated number order integral or differential supervisors. It is a presently debated problem with scientists since many multidimensional operations could be formed through conformable derivatives in numerous disciplines of implemented science which as solid-state physics, fractional dynamics, fluid mechanics, control theory, geochemistry, plasma physics, astrophysics, system identification, chemical physics, and many more. The various appeals of conformable derivatives show that there is an essential requirement for better numerical and analytical algorithms including real objects and methods. Consequently, the examination of the soliton solutions for nonlinear conformable models expresses a critical function for the research of nonlinear wave phenomena. Numerous mathematical procedures have been presented to get results of NLCMs, for example, homotopy perturbation method [1], residual power series method [2], Shifted Jacobi spectral collocation method [3], reproducing kernel Hilbert space method [4], modified generalized Taylor fractional series method [5], the improved fractional Riccati extension scheme [6], method of separation variables [7], generalized (G'/G)-extension scheme [8], Chebyshev collocation way [9], rational (G'/G)-extension scheme [10], the first integral way [11], modified exp-task way [12], variational iteration method [13], modified Khater method [14], and iterative reproducing kernel Hilbert space approach [15].

The paper applied the GK method [16] to derive the different types of solitary wave structures for the conformable Duffing equation (DE) [8], the conformable Riccati equation (RE) [8], and the conformable biological population model (BPM)

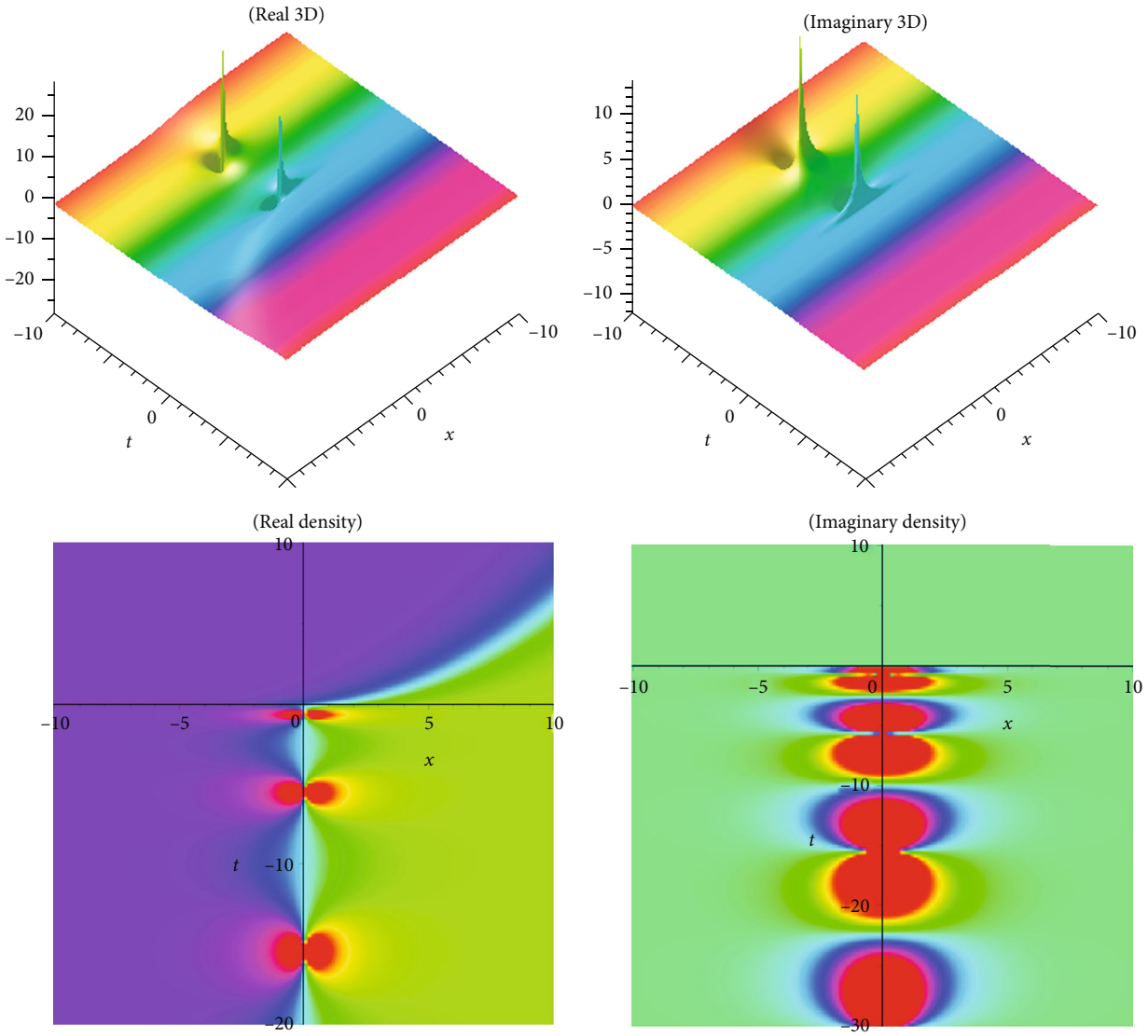

Figure 1: 3D and density pictures of $Z_1(\xi)$ for $p = 1$, $B_0 = 0.6$, $c = -2$, and $\varpi = 0.5$.

[6, 10]; in [17], it is examined time-fractional biological population model and gained some new solitary wave structures through the modified (G'/G)-expansion method.

Firstly, the conformable RE [8] is as follows:

$$\frac{\partial^{\varpi} Z(x,t)}{\partial t^{\varpi}} = \beta_0 + \beta_1 Z(x,t) + \beta_2 Z^2(x,t), t > 0, \varpi \in (0,2), \tag{1}$$

where

$$\frac{\partial^{\varpi} Z(x,t)}{\partial t^{\varpi}} = lim_{\varepsilon \longrightarrow 0} \frac{Z\left(x, t + \varepsilon t^{1-\varpi}\right) - Z(x,t)}{\varepsilon}, t > 0, \varpi \in (0,1), \tag{2}$$

and β_0, β_1, and β_2 are constants. If $\varpi = 1$, then the Eq. (1) decreases to the classical RE. The significance of the Eq. (1) normally occurs in optimal control difficulties. The result of the linear-quadratic optimal control depends on a RE, which has to be observed for the control rule's all-time horizon. The present research on conformable RE leads to concentrate on accurate values for ϖ. $\varpi = 1/2$ is remarkably familiar. This is because, in classical conformable calculus, numerous of the models were improved applying these appropriate orders of derivatives. In current attention, many further usual values of the ϖ arrive in the models. Consequently, one requires to analyze mathematical processes to determine the RE of arbitrary order. Inserting appropriate values of $\beta_0 = 1$, $\beta_1 = 0$, and $\beta_2 = -1$ in (1), the general conformable RE uses

$$\frac{\partial^{\varpi} Z(x,t)}{\partial t^{\varpi}} + Z^2(x,t) - 1 = 0, t > 0, \varpi \in (0,1). \tag{3}$$

Eq. (3) exposes numerous charming soliton structures that have not yet been confirmed. In the equations modeling

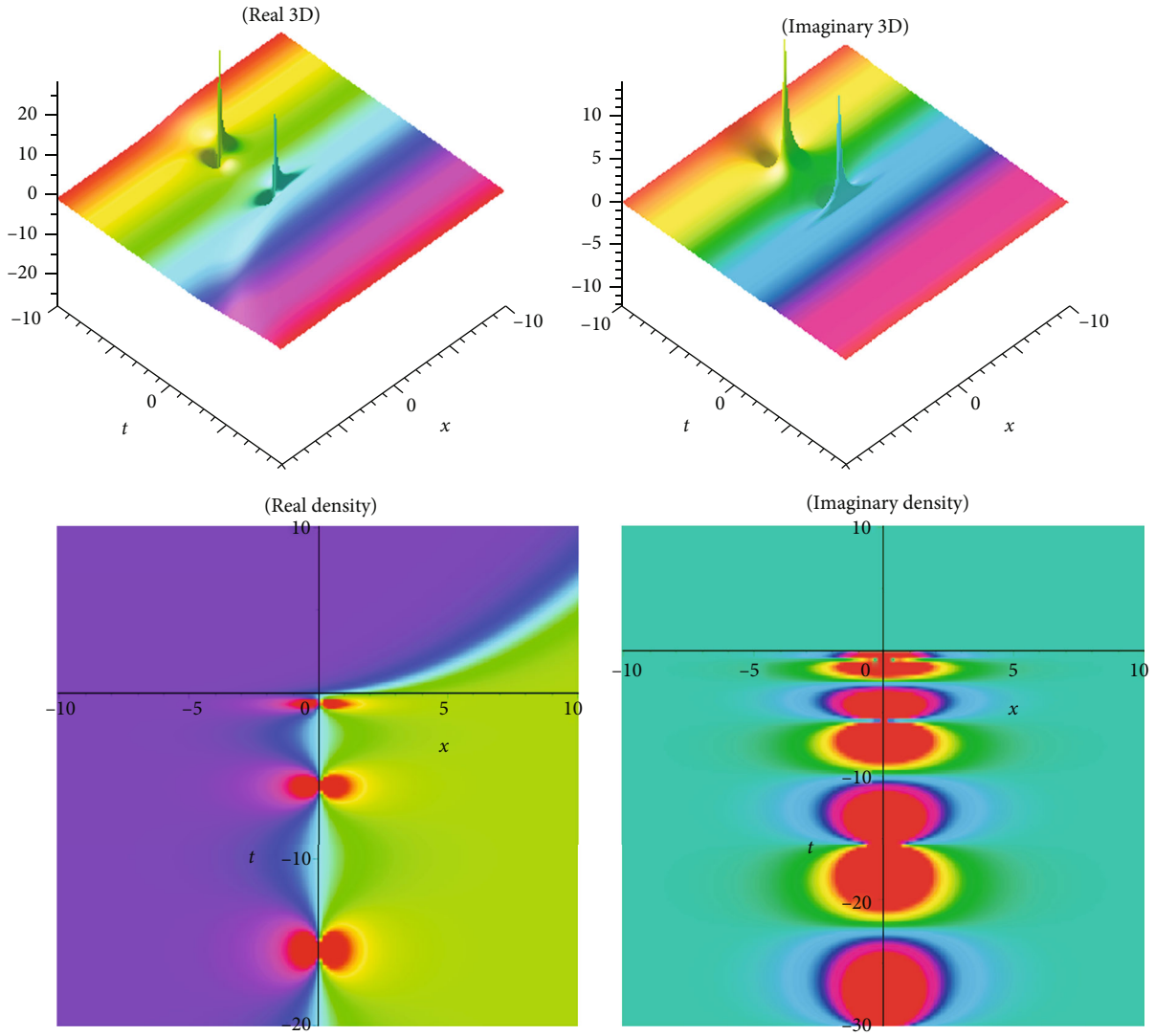

FIGURE 2: 3D and density pictures of $Z_2(\xi)$ for $p = 100$, $B_0 = -10$, $c = -2$, and $\varpi = 0.5$.

wave phenomena, one of the key goals is the soliton structures, maintaining results of the constant form with a constant velocity. Soliton constructions, together with their result definitions, are in explicit or implicit ways and are pretty fantastic from the perspective of applications. Such a diversity of soliton constructions is instantly named because they do not exchange their sketches when propagation. Our attention in this investigation is to analyze the soliton constructions; the solitary waves enclosed through asymptotically zero at a substantial distance, traveling waves, the kink variety waves, and the periodic waves, which increase or run down from one asymptotic state to other states.

Secondly, the conformable DE [8] is as follows:

$$\frac{\partial^{2\varpi} V(x,t)}{\partial t^{2\varpi}} + \gamma_0 V(x,t) + \gamma_1 V^3(x,t) = 0, t > 0, \varpi \in (0,1), \tag{4}$$

where ϖ is a conformable constant. In the model, the damping force is proportionate to the initial order derivative of the displacement. Numerous prosperous importance in manufacturing engineering have been informed by maintaining the integral form damping to a conformable form one because it can describe the compound frequency of damping materials. The display of fusion phenomena and the manifestation of fission aspects for solitons have been introduced theoretically and experimentally.

Finally, the conformable BPM [6, 10] is as follows:

$$D_t^{\varpi} W - D_x^2 W - D_y^2 W - S_1\left(W^2 - S_2\right) = 0. \tag{5}$$

Here W describes the population density, S_1 and S_2 are free parameters, and $s_1(W^2 - s_2)$ expresses the population supply owing to births and deaths. The solutions obtained exhausting the mentioned procedure can be expressed in the form of trigonometric, hyperbolic, and rational type

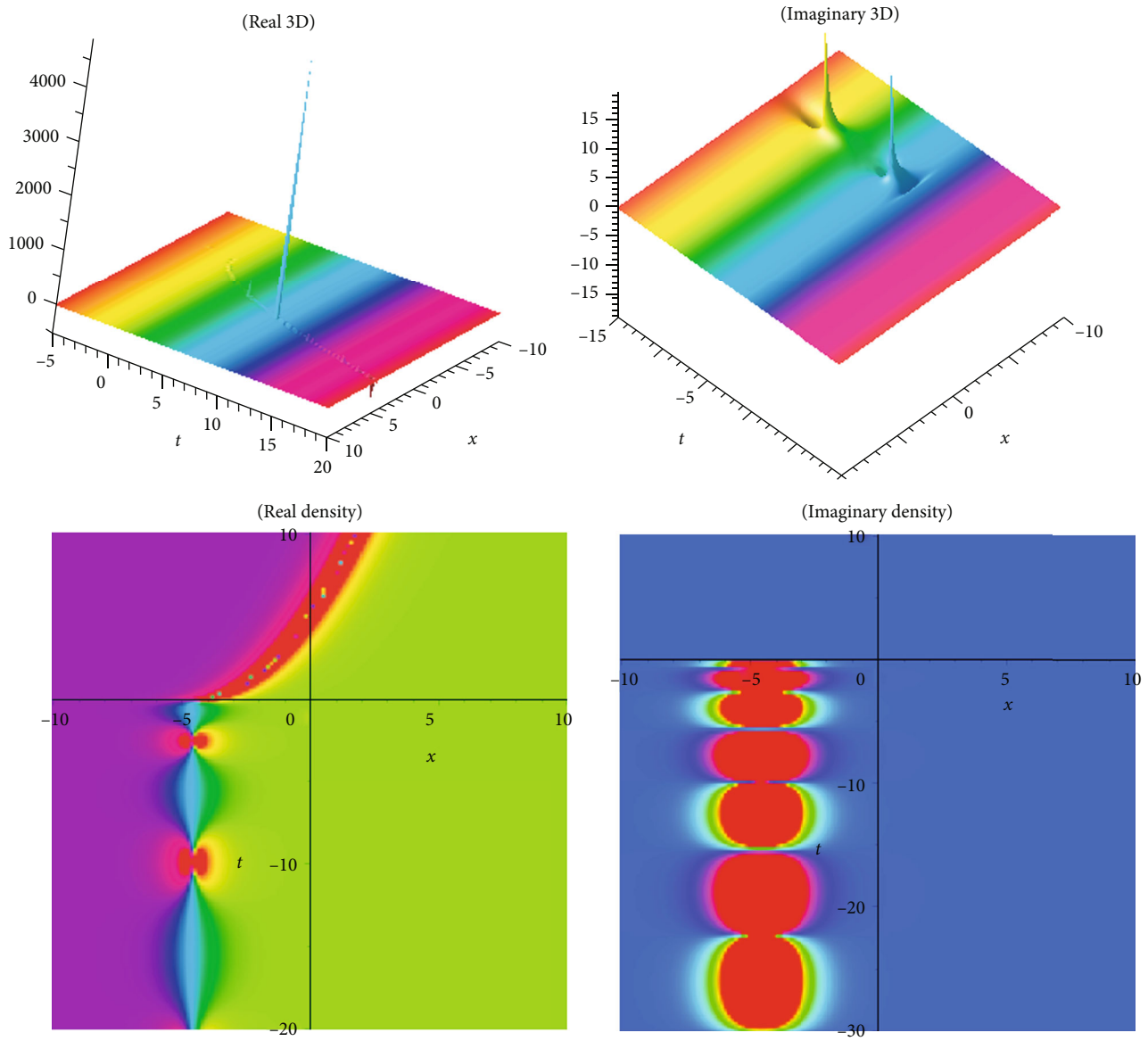

FIGURE 3: 3D and density pictures of $Z_3(\xi)$ for $p = 100$, $B_0 = 100$, $c = -1$, and $\varpi = 0.5$.

functions. These arrangements of the solutions are reasonable for revising convinced real type physical phenomena. However, there are various types of models that are useful for computing different models, for instance, ranking extreme efficient decision?, new extended rational SGEEM for construction of optical solitons?, the time nonlinear fractional generalized equal width model arising in shallow water channel?, an efficient alternating direction explicit method?, the variable coefficients generalized shallow water wave equation?, M-fractional solitary wave solutions and convergence analysis for Boussinesq equations?, the solving the Volterra integral equations with a weakly singular kernel? and an analytical analysis to solve the fractional differential equations? In the literature, these nonlinear model of equations for natural models are well used. These nonlinear models can be used alone or in combination to model physical processes relevant to engineering, technology, and sciences.

2. Glimpse of the GK Method

Step 1. Suppose a conformable PDE for $W(x, t)$ takes the form

$$R\left(\frac{\partial^{\varpi} W}{\partial t^{\varpi}}, \frac{\partial W}{\partial t}, \frac{\partial^{2\varpi} W}{\partial t^{2\varpi}}, \frac{\partial^2 W}{\partial t^2}, \cdots\right) = 0, \tag{6}$$

where R represents a polynomial in W, and $\partial^{\varpi} W/\partial t^{\varpi}$ and $\partial^{2\varpi} W/\partial t^{2\varpi}$ are conformable derivatives of W. (7).

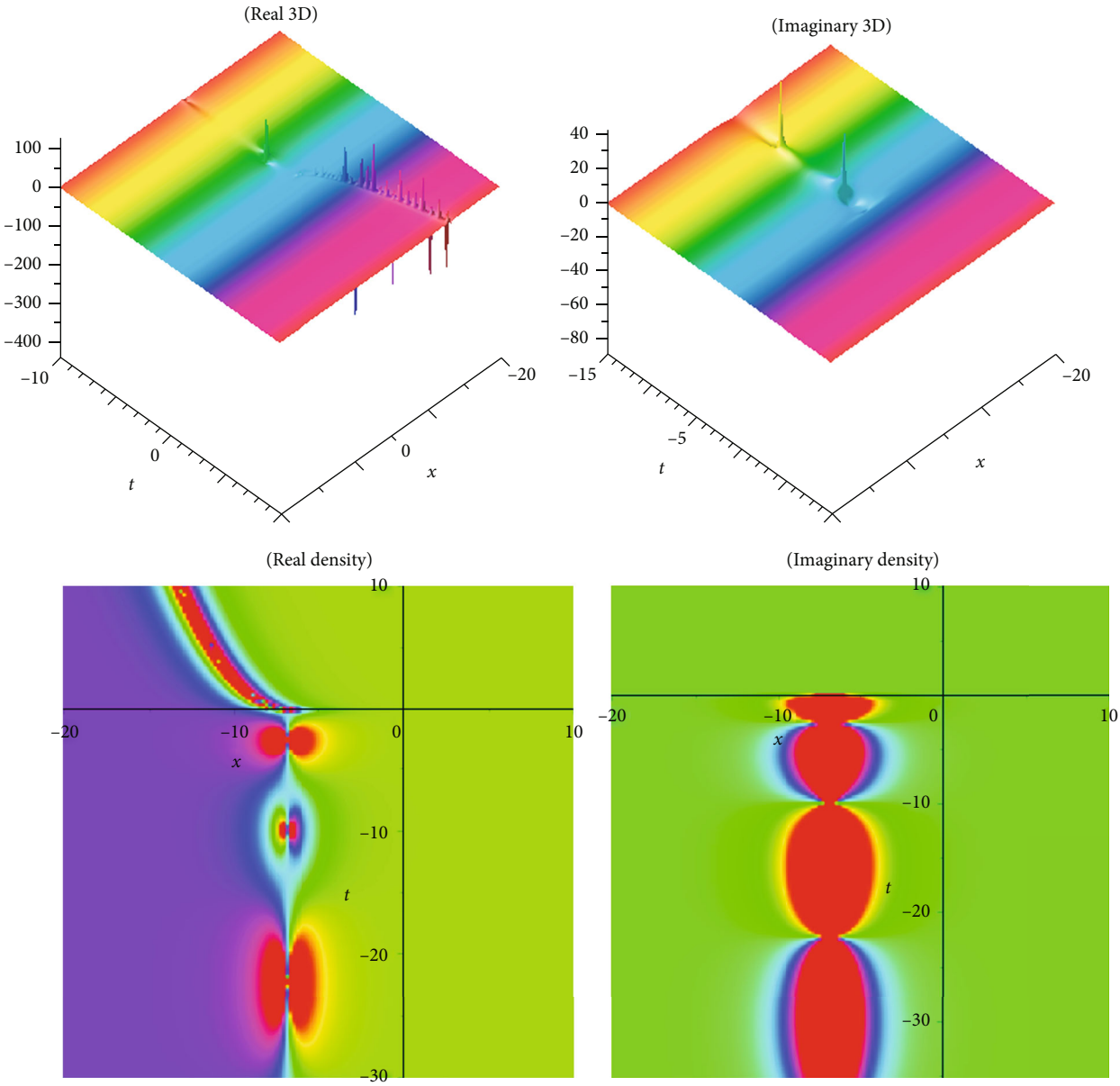

FIGURE 4: 3D and density pictures of $Z_4(\xi)$ for $p = -1000$, $B_0 = -5000$, $c = 1$, and $\varpi = 0.5$.

To locate the transformation of Eq. (6),

$$W = W(x,t) = W(\xi), \xi = x - \frac{ct^{\varpi}}{\varpi}. \tag{7}$$

From Eq. (6) and Eq. (7), we locate the following ODE:

$$S\left(W, W', W'', W''', \cdots\right) = 0. \tag{8}$$

Step 2. Compute M and N on Eq. (8).

Step 3. We examine the following:

$$W(\xi) = \frac{\sum_{i=0}^{N} A_i \Phi^i}{\sum_{j=0}^{M} B_j \Phi^j}. \tag{9}$$

Here, A_i and B_j are constants as well as $A_N, B_M \neq 0$ and Φ:

$$\Phi'(\xi) = \Phi^2(\xi) - \Phi(\xi). \tag{10}$$

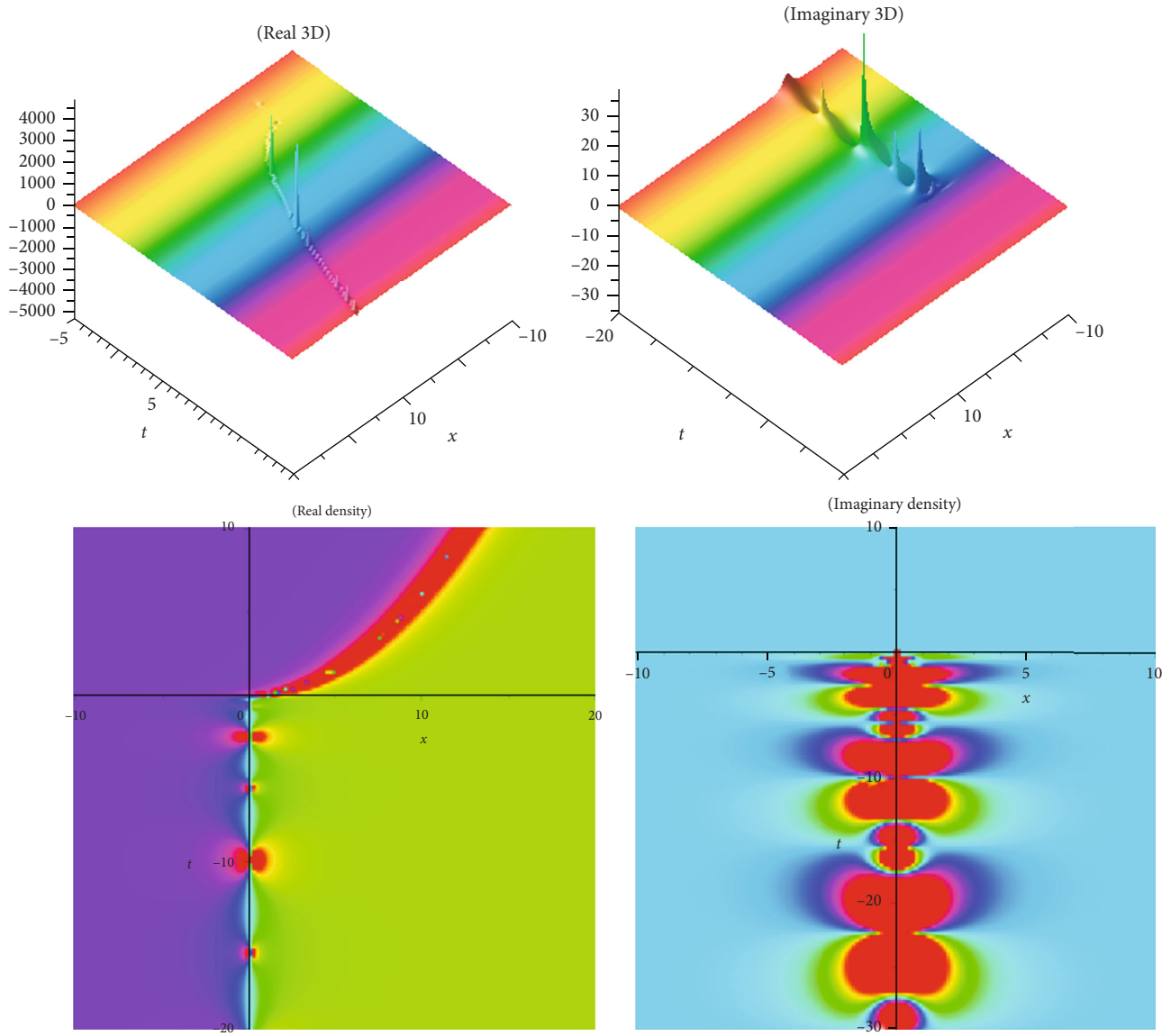

Figure 5: 3D and density pictures of $V_1(\xi)$ for $p = 1$, $a = -0.5$, $b = -0.3$, $\varpi = 0.5$, and $B_1 = -0.6$.

Eq. (10) provides

$$\Phi(\xi) = \frac{1}{1 + pe^{\xi}}. \tag{11}$$

Step 4. Compute N and M in Eq. (9) with the nonlinear term of $W(\xi)$ in Eq. (6) or Eq. (8).

Step 5. From Eq. (9), Eq. (8), and Eq. (11), we could be solved to determine $\Phi(\xi)$ through MAPLE.

3. Solitons to the Conformable RDE

Using $\xi = x + (ct^{\varpi}/\varpi)$, then Eq. ((1)) changes for $Z(x, t) = Z(\xi)$:

$$cZ'2(\xi) - 1 = 0. \tag{12}$$

From Eq. (12), $(Z'(\xi)$ and $Z^2(\xi)) \Rightarrow (2(N - M) = N - M + 1) \Rightarrow (N = M + 1)$. Setting $M = 1$, then $N = 2$. Therefore, we get

$$Z(\xi) = \frac{A_0 + A_1\Phi + A_2\Phi^2}{B_0 + B_1\Phi}. \tag{13}$$

Through Eq. (13) and Eq. (12), we find the following: The first set:

$$c = -2, A_0 = -B_0, A_1 = -B_1 + 2B_0, A_2 = 2B_1, \tag{14}$$

where B_0 and B_1 are constants. From the first set, Eq. (13)

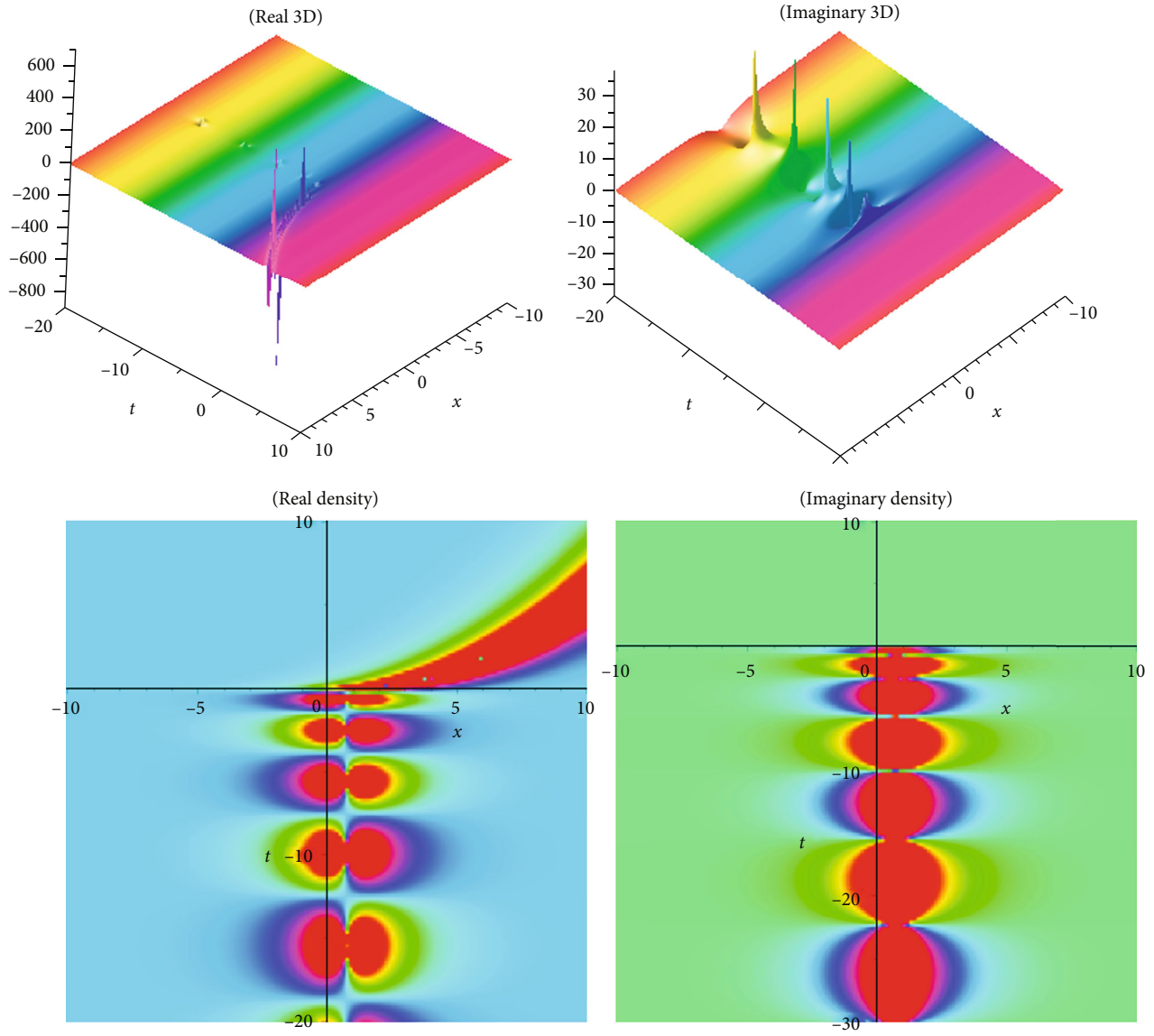

FIGURE 6: 3D and density pictures of $V_2(\xi)$ for $p = -0.5$, $a = -0.03$, $b = -0.005$, $\varpi = 0.5$, and $B_1 = -0.5$.

and Eq. (12), we have

$$Z_1(\xi) = \frac{-B_0 + (-B_1 + 2B_0) \times \left(1/1 + pe^{x+ct^{\varpi}/\varpi}\right) + 2B_1\left(1/1 + pe^{x+ct^{\varpi}/\varpi}\right)^2}{B_0 + B_1\left(1/1 + pe^{x+ct^{\varpi}/\varpi}\right)}. \tag{15}$$

The second set:

$$c = 2, A_0 = B_0, A_1 = -2B_0 + 2B_1, A_2 = -2B_1, \tag{16}$$

where B_0 and B_1 are constants.
Similarly, we get

$$Z_2(\xi) = \frac{B_0 + (-2B_0 + 2B_1) \times \left(1/1 + pe^{x+ct^{\varpi}/\varpi}\right) - 2B_1\left(1/1 + pe^{x+ct^{\varpi}/\varpi}\right)^2}{B_0 + B_1\left(1/1 + pe^{x+ct^{\varpi}/\varpi}\right)}. \tag{17}$$

The third set:

$$c = -1, A_0 = -B_0, A_1 = 2B_0, A_2 = -2B_0, B_1 = -2B_0, \tag{18}$$

where B_0 is constants. Similarly, we get

$$Z_3(\xi) = \frac{-B_0 + 2B_0\left(1/1 + pe^{x+ct^{\varpi}/\varpi}\right) - 2B_0\left(1/1 + pe^{x+ct^{\varpi}/\varpi}\right)^2}{B_0 - 2B_0\left(1/1 + pe^{x+ct^{\varpi}/\varpi}\right)}. \tag{19}$$

The fourth set:

$$c = 1, A_0 = B_0, A_1 = -2B_0, A_2 = 2B_0, B_1 = -2B_0, \tag{20}$$

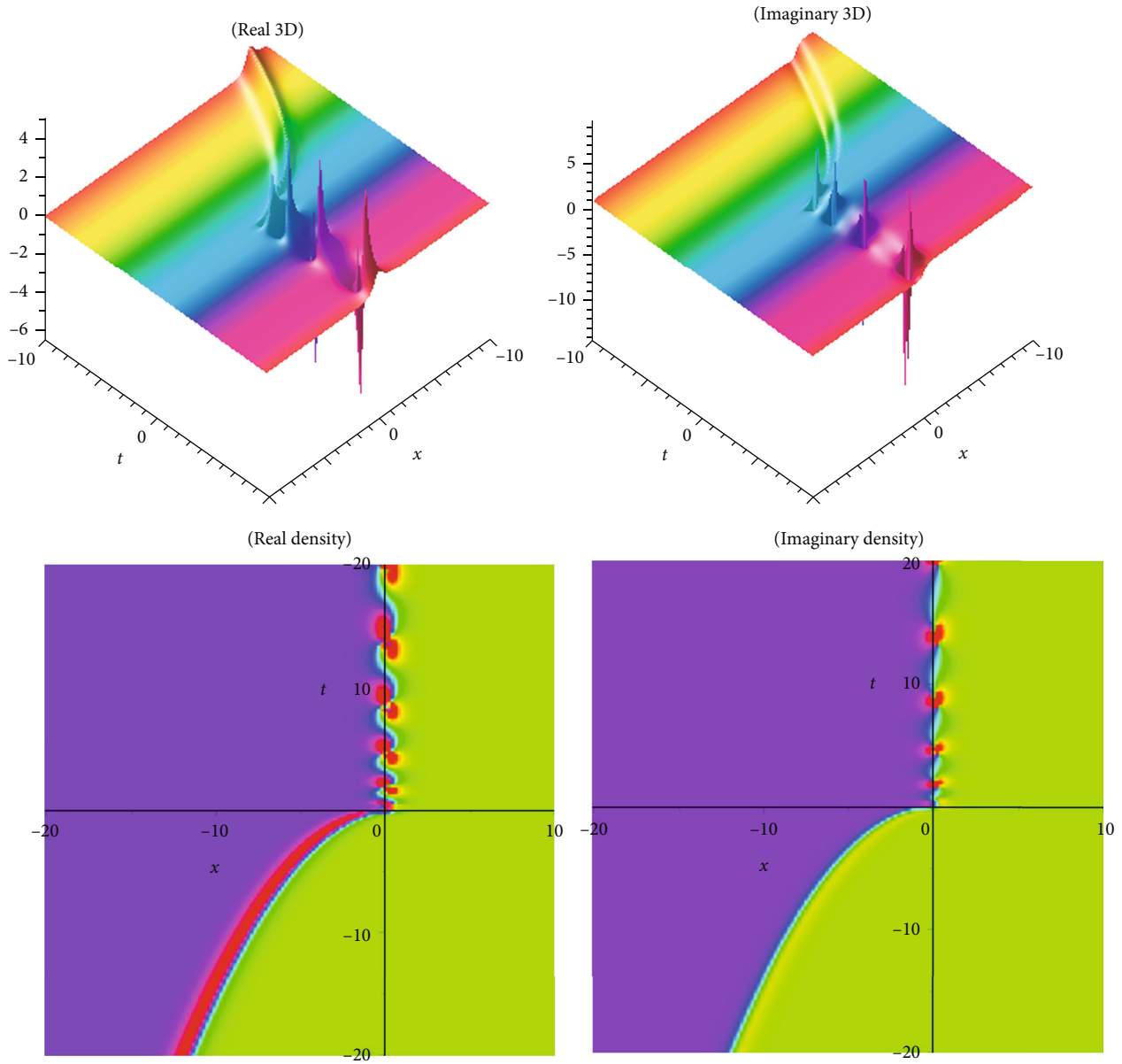

FIGURE 7: 3D and density pictures of $W_1(\xi)$ for $p = 1$, $\varpi = 1/2$, $y = -100$, $B_1 = 0.6$, $A_1 = 2$, $S_1 = 2$, $S_2 = 1$, and $S_3 = 3$.

where B_0 is constants. Similarly, we get:

$$Z_4(\xi) = \frac{B_0 - 2B_0\left(1/1 + pe^{x+ct^{\varpi}/\varpi}\right) + 2B_0\left(1/1 + pe^{x+ct^{\varpi}/\varpi}\right)^2}{B_0 - 2B_0\left(1/1 + pe^{x+ct^{\varpi}/\varpi}\right)}. \tag{21}$$

4. Solitons to the Conformable DE

Using $\xi = x + (ct^{\varpi}/\varpi)$, then Eq. (4) changes for $V(x,t) = V(\xi)$:

$$c^2 V''3(\xi) = 0. \tag{22}$$

From Eq. (22), $(V''(\xi)$ and $V^3(\xi)) \Rightarrow (3(N-M) = N - M+2) \Rightarrow (N = M+1)$. Setting $M = 1$, then $N = 2$. Therefore, we get

$$V(\xi) = \frac{A_0 + A_1\Phi + A_2\Phi^2}{B_0 + B_1\Phi}. \tag{23}$$

Through Eq. (23) and Eq. (22), we have the following sets:

The first set:

$$c = \sqrt{-a}, A_0 = 0, A_1 = -B_1\sqrt{\frac{2a}{b}}, A_2 = B_1\sqrt{\frac{2a}{b}}, B_0 = -\frac{1}{2}B_1. \tag{24}$$

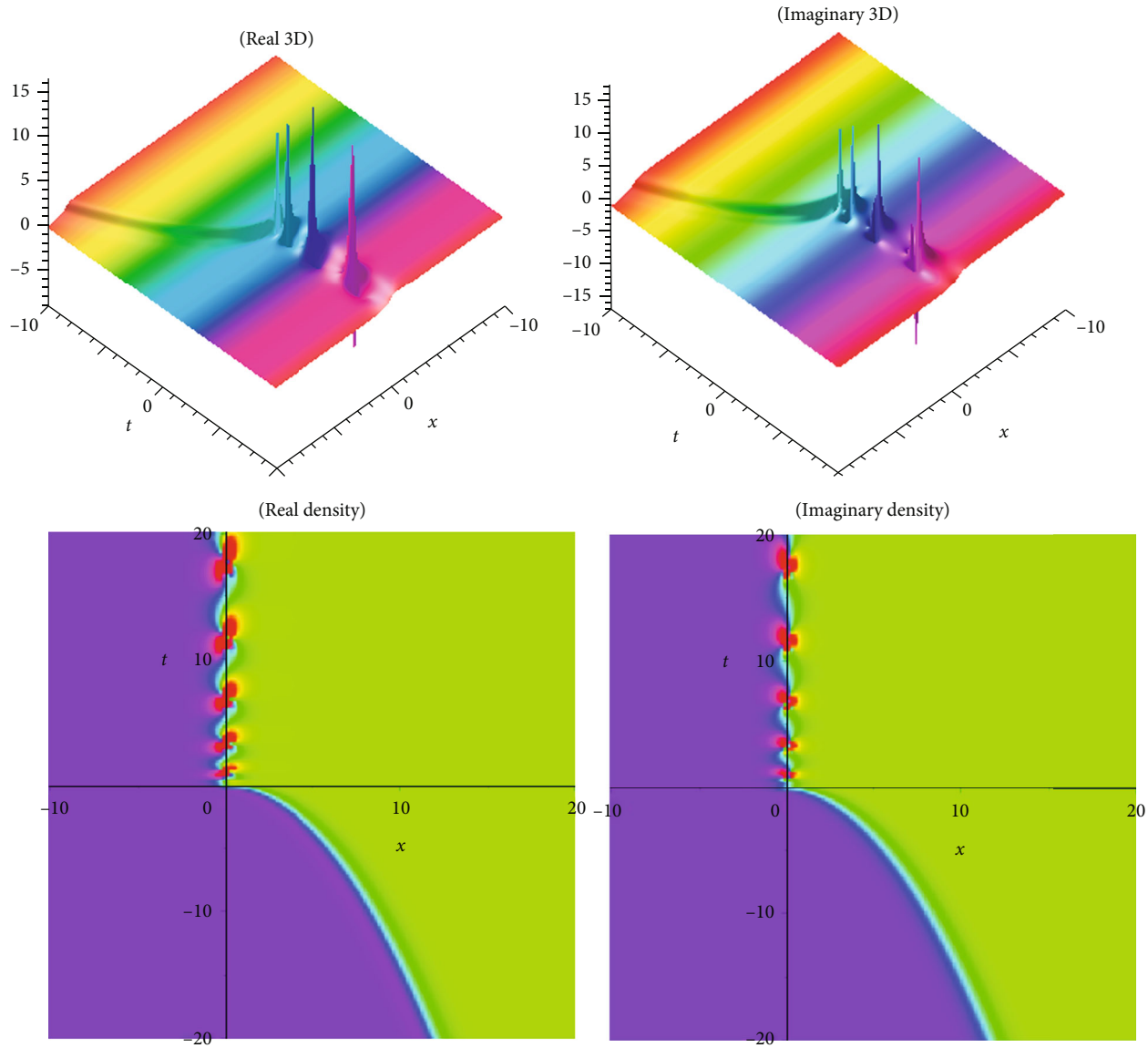

Figure 8: 3D and density pictures of $W_2(\xi)$ for $p = -10$, $\varpi = 1/2$, $y = 1$, $B_1 = 0.6$, $A_1 = 2$, $S_1 = 2$, $S_2 = 5$, and $S_3 = 3$.

From the first set, Eq. (13) and Eq. (12), we have

$$V_1(\xi) = \frac{-B_1\sqrt{2a/b}\left(1/1 + pe^{x+ct^{\varpi}/\varpi}\right) + B_1\sqrt{2a/b}\left(1/1 + pe^{x+ct^{\varpi}/\varpi}\right)^2}{-1/2B_1 + B_1\left(1/1 + pe^{x+ct^{\varpi}/\varpi}\right)}. \tag{25}$$

The second set:

$$c = -\sqrt{-a}, A_0 = 0, A_1 = B_1\sqrt{\frac{2a}{b}}, A_2 = -B_1\sqrt{\frac{2a}{b}}, B_0 = -\frac{1}{2}B_1. \tag{26}$$

Similarly, we get

$$V_2(\xi) = \frac{B_1\sqrt{2a/b}\left(1/1 + pe^{x+ct^{\varpi}/\varpi}\right) - B_1\sqrt{2a/b}\left(1/1 + pe^{x+ct^{\varpi}/\varpi}\right)^2}{-1/2B_1 + B_1\left(1/1 + pe^{x+ct^{\varpi}/\varpi}\right)}. \tag{27}$$

5. Solitons to the Conformable BPM

Let us consider the Eq. (5).

Making $W(x, y, t) = W(\xi), \xi = S_3(x + iy) - S_0 t^{\varpi}/\varpi$, and $i^2 = -1$ into the Eq. (5), we derive

$$S_0 W' - S_1\left(W^2 - S_2\right) = 0. \tag{28}$$

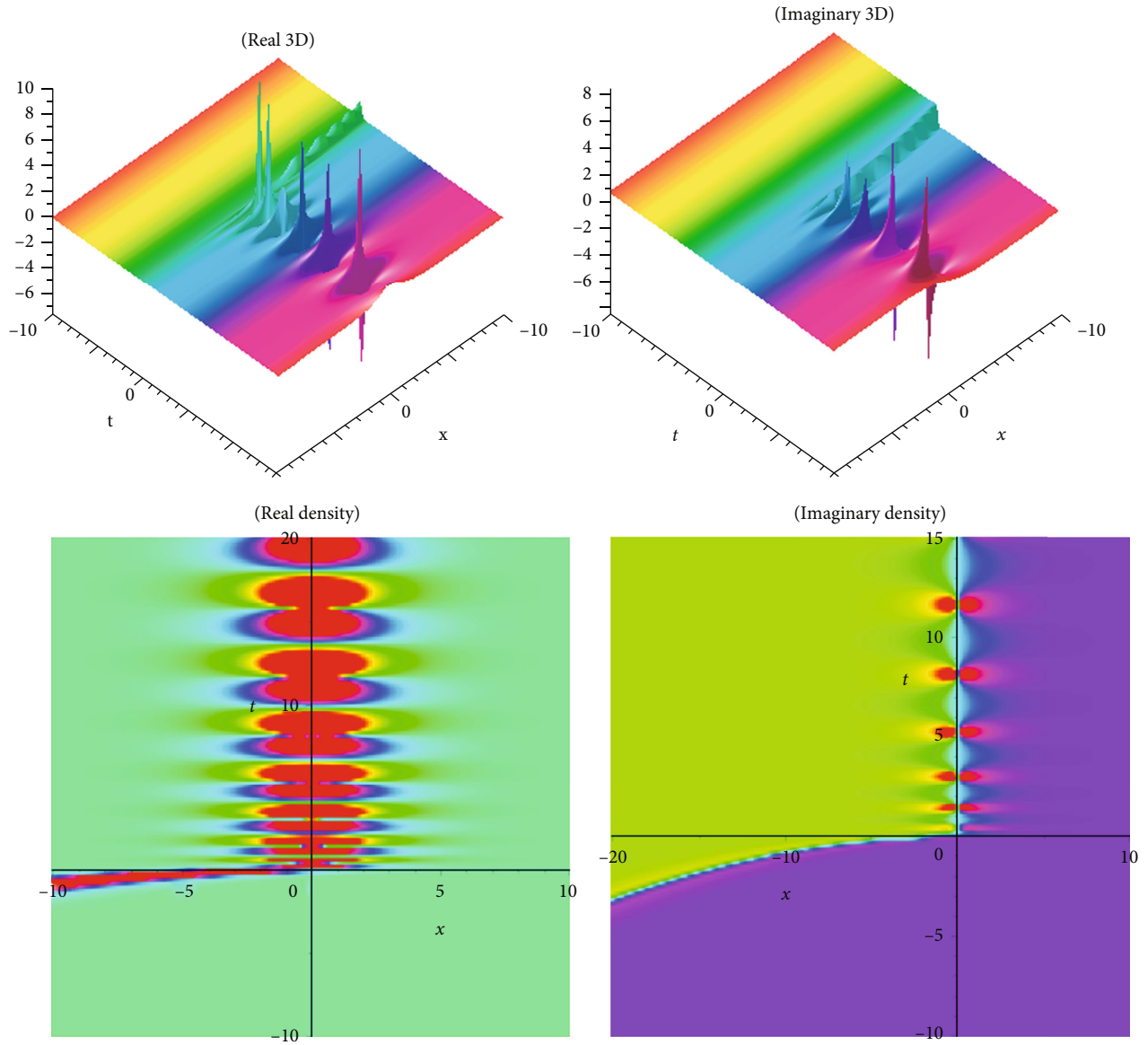

FIGURE 9: 3D and density pictures of $W_3(\xi)$ for $p = 1$, $\omega = 1/2$, $y = 1$, $B_1 = 0.6$, $S_1 = -2$, $S_2 = 0.5$, and $S_3 = 0.5$.

From Eq. (28), $(V''(\xi)$ and $V^3(\xi)) \Rightarrow (3(N-M) = N - M + 2) \Rightarrow (N = M + 1)$. Setting $M = 1$, then $N = 2$. Therefore, we get

$$W(\xi) = \frac{A_0 + A_1\Phi + A_2\Phi^2}{B_0 + B_1\Phi}. \tag{29}$$

Through Eq. (29) and Eq. (28), we have the following sets:

The first set:

$$S_0 = 2\sqrt{-S_2}S_1, A_0 = -\frac{\sqrt{-S_2}A_1 - B_1S_2}{2\sqrt{-S_2}}, A_2 = 2\sqrt{-S_2}B_1, B_0 = \frac{\sqrt{-S_2}B_1 + A_1}{2\sqrt{-S_2}}. \tag{30}$$

From the first set, Eq. (29) and Eq. (28), we have

$$W_1(\xi) = \frac{\left(\sqrt{-S_2}A_1 - B_1S_2/2\sqrt{-S_2}\right) + A_1\left(1/1 + pe^{S_3(x+iy)-S_0t^{\varpi}/\varpi}\right) + 2\sqrt{-S_2}B_1\left(1/1 + pe^{S_3(x+iy)-S_0t^{\varpi}/\varpi}\right)^2}{\left(\sqrt{-S_2}B_1 + A_1/2\sqrt{-S_2}\right) + B_1\left(1/1 + pe^{S_3(x+iy)-S_0t^{\varpi}/\varpi}\right)}. \tag{31}$$

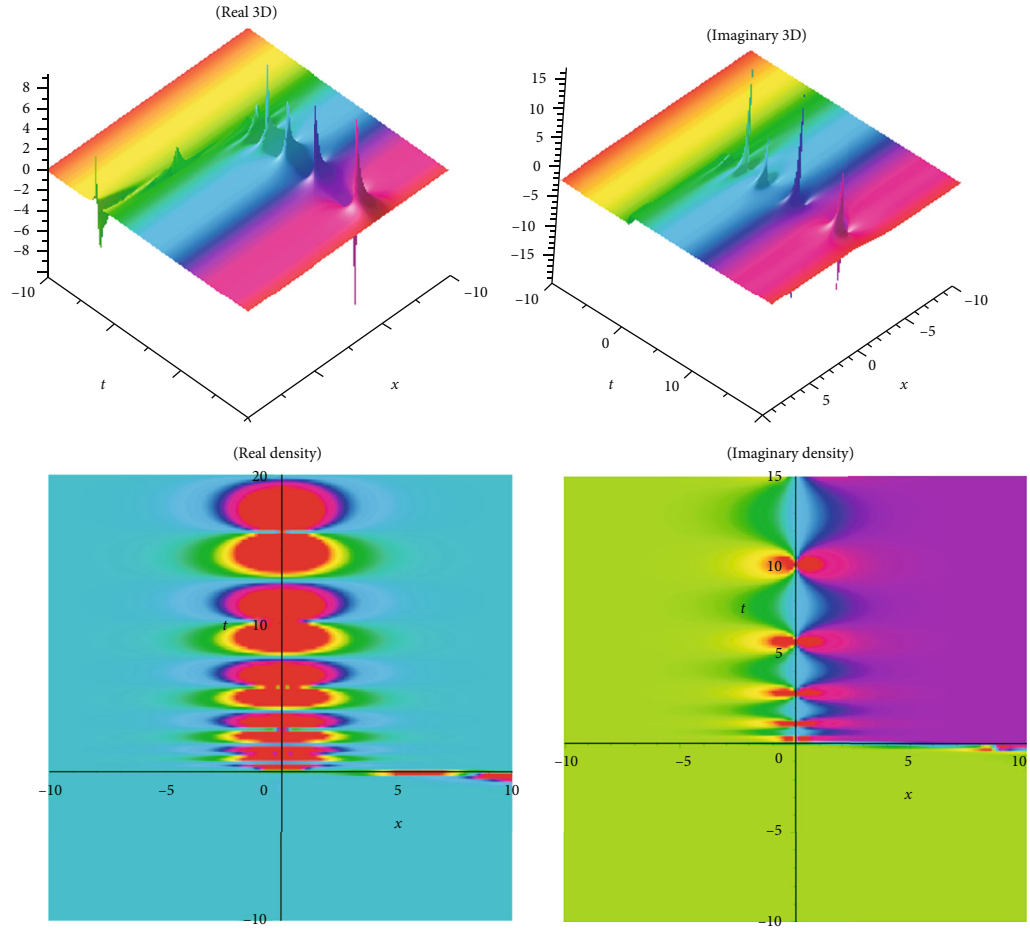

FIGURE 10: 3D and density pictures of $W_4(\xi)$ for $p = 1$, $\varpi = 1/3$, $y = 1$, $B_1 = 0.6$, $S_1 = -2$, $S_2 = 0.5$, and $S_3 = 0.5$.

The second set:

$$S_0 = -2\sqrt{-S_2}S_1, A_0 = \frac{-\sqrt{-S_2}A_1 - B_1S_2}{2\sqrt{-S_2}}, A_2 = -2\sqrt{-S_2}B_1, B_0 = \frac{-\sqrt{-S_2}B_1 + A_1}{2\sqrt{-S_2}}. \tag{32}$$

Similarly, we get

$$W_2(\xi) = \frac{\left(-\sqrt{-S_2}A_1 - B_1S_2/2\sqrt{-S_2}\right) + A_1\left(1/1 + pe^{S_3(x+iy)-S_0t^{\varpi}/\varpi}\right) - 2\sqrt{-S_2}B_1\left(1/1 + pe^{S_3(x+iy)-S_0t^{\varpi}/\varpi}\right)^2}{\left(-\sqrt{-S_2}B_1 + A_1/2\sqrt{-S_2}\right) + B_1\left(1/1 + pe^{S_3(x+iy)-S_0t^{\varpi}/\varpi}\right)}. \tag{33}$$

The third set:

$$S_0 = -2\sqrt{-S_2}S_1, A_0 = \frac{B_1S_2}{2\sqrt{-S_2}}, A_1 = \sqrt{-S_2}B_1, A_2 = -\sqrt{-S_2}B_1, B_0 = -\frac{B_1}{2}. \tag{34}$$

Similarly, we get

$$W_3(\xi) = \frac{\left(B_1 S_2/2\sqrt{-S_2}\right) + \sqrt{-S_2}B_1\left(1/1 + pe^{S_3(x+iy)-S_0 t^{\omega}/\omega}\right) - \sqrt{-S_2}B_1\left(1/1 + pe^{S_3(x+iy)-S_0 t^{\omega}/\omega}\right)^2}{-(B_1/2) + B_1\left(1/1 + pe^{S_3(x+iy)-S_0 t^{\omega}/\omega}\right)}. \tag{35}$$

The fourth set:

$$S_0 = 2\sqrt{-S_2}S_1, A_0 = -\frac{B_1 S_2}{2\sqrt{-S_2}}, A_1 = -\sqrt{-S_2}B_1, A_2 = \sqrt{-S_2}B_1, B_0 = -\frac{B_1}{2}. \tag{36}$$

Similarly, we get

$$W_4(\xi) = \frac{-B_1 S_2/2\sqrt{-S_2} - \sqrt{-S_2}B_1\left(1/1 + pe^{S_3(x+iy)-S_0 t^{\omega}/\omega}\right) + \sqrt{-S_2}B_1\left(1/1 + pe^{S_3(x+iy)S_0 t^{\omega}/\omega}\right)^2}{-(B_1/2) + B_1\left(1/1 + pe^{S_3(x+iy)-S_0 t^{\omega}/\omega}\right)}. \tag{37}$$

The physical meaning of solutions is as follows: this segment will examine the physical explanation of the time-fractional biological population model of the acknowledged exact influencing wave equation. The three-dimensional (3D) charts and density plots including real and imaginary parts of the newest fractional BPM equations' travelling wave solutions are discussed in this subsection. A three-dimensional plot depicts the extent of divergence across time or relates many wave issues. Wave facts are arranged in a logical order with equally spaced disturbances and connected by a line to show the relationships between them. The diagram's pictorial value is enhanced by the 3D style. The density plot and 3D plot are designed to show the low and high frequency and amplitude extremely clearly.

6. Conclusion

In the current work, we have secured the exact traveling wave answers in the novel method, for instance, kink variety traveling wave answers, double soliton, multiple solitons, periodic, and singular soliton of the Eqs. (1), (4), and (5). The two models' established answers, as mentioned above, are applicable to search the fusion and fission aspects. This natural phenomenon happens for solitons, electromagnetic interactions, scalar electrodynamics, quantum relativistic one-particle theory, relativistic energy-momentum relation, etc. The magnitude of the Eq. (1) usually rises in determining the optimal control difficulties. In the echo region, the oscillation of vibration depends on the damping exponent in a nontrivial way. So, to reduce severe fluctuation is an introductory presentation of the Eq. (4). The picture is a crucial device for information and to express the answers to the difficulties lucidly. When performing the calculation in daily life, we need a fundamental knowledge of building graphs. Subsequently, the graphical displays of a few answers are illustrated in Figures 1–10, respectively. We displayed Figures 1–10, respectively, for a few of the derived answers to reveal more features for the prescribed model. The GK method's performance is more accessible and reliable than the other approaches to define the exact answers derived in this research. The technique can be significant for further examining distinct conformable PDEs in high energy physics, mathematical physics, quantum gravity, and numerous nonlinear physics branches. It is obvious that the technique we suggest is successful, dependable, and easy to use, and that it provides enough well-matched answers for NLFPDEs that emerge in engineering, applied mathematics, and mathematical physics.

Data Availability

The data used to support the findings of this study are included within the article.

Conflicts of Interest

The authors declare that they have no conflicts of interest.

References

[1] S. Bushnaq, S. Ali, K. Shah, and M. Airf, "Exact solution to non-linear biological population model with fractional order," *Thermal Science*, vol. 22, Supplement 1, pp. 317–327, 2018.

[2] A. Omar, "Application of residual power series method for the solution of time-fractional Schrödinger equations in one-dimensional space," *Fundamenta Informaticae*, vol. 166, no. 2, pp. 87–110, 2019.

[3] E. H. Doha, M. A. Abdelkawy, A. Z. M. Amind, and D. Baleanu, "Shifted Jacobi spectral collocation method with convergence analysis for solving integro-differential equations and system of integro-differential equations," *Nonlinear Analysis: Modelling and Control*, vol. 24, no. 3, pp. 332–352, 2019.

[4] A. Omar, "Modulation of reproducing kernel Hilbert space method for numerical solutions of Riccati and Bernoulli equations in the Atangana-Baleanu fractional sense," *Chaos, Solitons and Fractals*, vol. 125, pp. 163–170, 2019.

[5] A. Khalouta and A. Kadem, "A new numerical technique for solving Caputo time-fractional biological population equation," *AIMS Mathematics*, vol. 4, no. 5, pp. 1307–1319, 2019.

[6] E. A. B. A. Salam and E. A. E. Gumma, "Analytical solution of nonlinear space-time fractional differential equations using the improved fractional riccati expansion method," *Ain Shams Engineering Journal*, vol. 6, no. 2, pp. 613–620, 2015.

[7] C. Wu and W. Rui, "Method of separation variables combined with homogenous balanced principle for searching exact solutions of nonlinear time-fractional biological population model," *Communications in Nonlinear Science and Numerical Simulation*, vol. 63, pp. 88–100, 2018.

[8] M. A. Akbar, N. H. M. Ali, and R. Roy, "Closed form solutions of two time fractional nonlinear wave equations," *Results in Physics*, vol. 9, pp. 1031–1039, 2018.

[9] M. M. Khader and K. M. Saad, "A numerical study by using the Chebyshev collocation method for a problem of biological invasion: fractional Fisher equation," *International Journal of Biomathematics*, vol. 11, no. 8, p. 1850099, 2018.

[10] M. A. Akbar, N. H. M. Ali, and M. T. Islam, "Multiple closed form solutions to some fractional order nonlinear evolution equations in physics and plasma physics," *AIMS Mathematical*, vol. 4, no. 3, pp. 397–411, 2019.

[11] O. Kolebaje, E. Bonyah, L. Mustapha, Department of Physics, Adeyemi College of Education, Ondo, Nigeria, Department of Mathematics Education, University of Education, Winneba, (Kumasi campus), Ghana, and Department of Physical Sciences, Al-Hikmah University, Ilorin, Nigeria, "The first integral method for two fractional non-linear biological models," *Discrete Continuous Dynamical Systems-S*, vol. 12, no. 3, pp. 487–502, 2019.

[12] S. T. M. Din, A. Ali, and B. B. Mohsin, "On biological population model of fractional order," *International Journal of Biomathematics*, vol. 9, no. 5, p. 1650070, 2016.

[13] Y. Wang and J. Y. An, "Amplitude–frequency relationship to a fractional duffing oscillator arising in microphysics and tsunami motion," *Journal of Low Frequency Noise,Vibration and Active Control*, vol. 38, no. 3-4, pp. 1008–1012, 2019.

[14] R. A. M. Attia, D. Lu, and M. M. A. Khater, "Chaos and relativistic energy-momentum of the nonlinear time fractional Duffing equation," *Mathematical and Computational Applications*, vol. 24, no. 1, p. 10, 2019.

[15] M. G. Sakar, A. Akgül, and D. Baleanu, "On solutions of fractional Riccati differential equations," *Math Advances in Difference Equations*, vol. 2017, article 39, 2017.

[16] A. Gaber, A. F. Aljohani, A. Ebaid, and J. T. Machado, "The generalized Kudryashov method for nonlinear space–time fractional partial differential equations of burgers type," *Nonlinear Dynamics*, vol. 95, no. 1, pp. 361–368, 2019.

[17] M. N. Alam, S. Aktar, and C. Tunc, "New solitary wave structures to time fractional biological population model," *Journal of Mathematical Analysis*, vol. 11, no. 3, pp. 59–70, 2020.